



## EFFECT OF SURFACE ROUGHNESS ON OIL-WATER SEPARATION FOR OIL SKIMMER

Mohamed Saiful Firdaus Hussin<sup>1</sup>, Azrul Abidin Zakaria<sup>3</sup>, Ridhwan Jumaidin<sup>1</sup>, Mastura Mohammad Taha<sup>1</sup>, Muhd Ridzuan Mansor<sup>2</sup>, Amir Abdullah Muhamad Damanhuri<sup>1</sup>, Mohd. Fariduddin Mukhtar<sup>1</sup>, Mohammad Khalid Wahid<sup>1</sup> and Mohd. Nazri Ahmad<sup>1</sup>

<sup>1</sup>Faculty of Mechanical and Manufacturing Engineering Technology, Malaysia

<sup>2</sup>Faculty of Mechanical Engineering Universiti Teknikal Malaysia Melaka, Hang Tuah Jaya, Durian Tunggal, Melaka, Malaysia

<sup>3</sup>Department of Mechanical Engineering, College of Engineering, Universiti Tenaga Nasional, Jalan IKRAM-UNITEN, Kajang, Selangor, Malaysia

E-Mail: [mohamed.saiful@utem.edu.my](mailto:mohamed.saiful@utem.edu.my)

### ABSTRACT

Uncontrolled production of fat, oil, & grease (FOG) in wastewater continues to increase each year as the number of restaurants increases. As wastes disposed directly into the drainage system, FOG may build up around the plumbing system of the wastewater system facility. Efficient development of the grease trap will reduce the impact of the problem and prevent the FOG contaminant in the sewage system. This research aimed to investigate the effect of surface roughness on oil skimming efficiency for the grease trap. Materials for oil skimmer were selected and characterized using water contact angle analysis, ImageJ software, scanning electron microscope (SEM), and profilometer. Materials were roughened by using 150 grid abrasive paper. It was found that roughness strongly influenced the wettability of the selected materials due to the air trap and its geometrical structure. The results revealed that acrylic skimmer is the most efficient compared to aluminium, paraffin, and polystyrene.

**Keywords:** surface roughness, oil skimmer, oil-water separation, retention time, wettability.

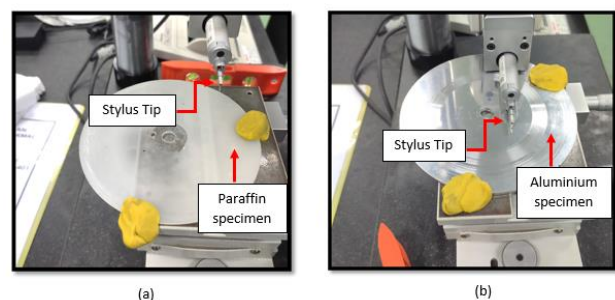
### INTRODUCTION

Food service establishments (FSE) produce a great amount of fat, oil, and grease (FOG) because they involved with the processes from collecting waste to waste treatment. Major factor contributes to the increasing number of FOG are people eating habits and increasing number of food outlets [1, 2]. Large industries such as palm oil mills also contribute to the increment of FOG in Malaysia. Based on the Malaysian Palm Oil Board (MPOB), the total plantation area of oil palm was 4, 487, 957 hectares in 2008 [3]. Untreated oil waste that came from FSE and large industries discharges to sewer lines reacts with the calcium in wastewater. Waste deposition reacts through saponification reaction that leads to the formation of the calcium-based fatty acid salts. The FOG deposits physical properties include metallic soaps consisting of (saturated) fatty acids and calcium [4-6]. The theory has been proved by He *et al.* [7] in an experiment using the same conditions as sewer lines. The most popular method to remove FOG used by FSE is using grease trap [8-10]. Oils often have a lower density than water, which is the reason that oil will float on water when the mix is allowed to settle for some time (also called retention time). Upper layer in wastewater contains floatable deposits such as FOG, and the middle layer usually filled with organic matter and the bottom layer consists of food particles [11, 12]. FOG components enter the sewer system in two different ways; directly release into sewer or grease trap failure. Grease trap failure means the grease trap cannot separate water and oil effectively. This phenome is due to the imbalance of pressure and flow between two compartments. The efficiency of skimmer in separating oil and water is still questionable. Thus, this paper will introduce a newly designed oil skimmer which

is expected to increase the efficiency of the skimming process with better oil-water separation percentage.

### METHODOLOGY

House of quality is applied to convert customer requirement into a proper plan, prioritizing steps from many options which the most important to the customer and do the realistic plan in connecting engineering element and product requirement [13-15]. A morphological chart is then used to generate ideas and concepts through visual selection [16-19]. Later, the Pugh method is used to evaluate and decide the best concepts generated by morphological chart [20, 21]. The material selection of these project is based on the wettability properties. Material characterization is then done by using water contact angle analysis, scanning electron microscope, and profilometer (SurfTest SJ-410).



**Figure-1.** Measuring method using surfTest SJ-410 for (a) Aluminium (b) Paraffin.



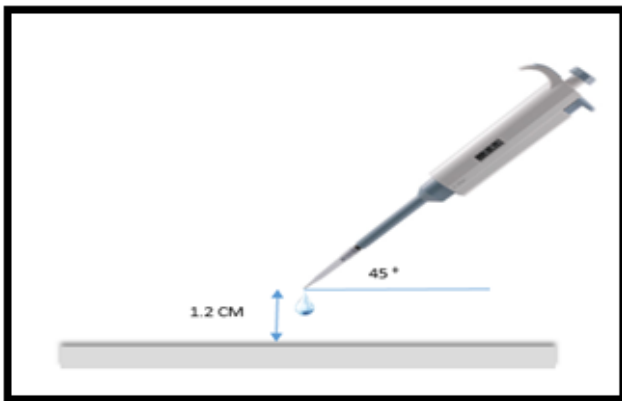
## RESULTS AND DISCUSSIONS

In most scenario, the factors that affect the wettability are surface porosity and roughness, as well as heterogeneity. Greater wetting propensity produces lower the contact angle or the surface tension. If the contact angle between a fluid and a solid is less than  $90^\circ$ , the liquid is damp and distributed over the substrate and the

phenomena is called hydrophilic. Meanwhile, if the contact angle is higher than  $90^\circ$ , the fluid may sit as a bead on the top of the surface and known as hydrophobic. Same goes for surface characteristics such as the roughness or topography. The contact angle of all tested materials is presented in Table-1.

**Table-1.** Water contact angle value.

Materials	Left	Right	Average	Sum of Water Contact Angle ( $^\circ$ )
Smooth Aluminium	67.70	69.80	68.75	68.74
	67.30	70.20	68.75	
	68.30	69.10	68.70	
Rough Aluminium	110.4	112.7	111.55	110.42
	109.1	109.8	109.45	
	107.3	113.2	110.25	
Smooth Paraffin	104.9	106.5	105.7	105.19
	104.2	105.3	104.8	
	103.9	106.3	105.1	
Rough Paraffin	119.1	117.7	118.4	117.48
	119.6	115.3	117.5	
	117.6	115.6	116.6	
Smooth Acrylic	68.1	69.3	68.70	68.1
	66.3	68.2	67.25	
	67.5	69.2	68.35	
Rough Acrylic	61.5	65.3	63.4	63.25
	60.3	67.5	63.9	
	59.8	65.1	62.5	
Smooth Polystyrene	71.1	73.2	72.15	71.9
	70.4	72.2	71.30	
	70.7	73.8	72.25	
Rough Polystyrene	87.6	86.1	86.85	86.67
	88.9	86.9	87.9	
	85.1	85.4	85.25	



**Figure-2.** Pipette distance between the substrate.

As the first experiment to study the surface roughness-dependence of contact angle, this experiment was able to test the surface roughness-dependence factors. The resistivity of distilled water is  $18.2 \text{ M}\Omega\text{-cm}$  to match that of the droplet to be added later. Initially, the distilled water was left out for 10 minutes to equalize the temperature between the surrounding and distilled water. After the substrate was placed, the droplet of distilled water was added on top of the substrate. Nevertheless, there is a tradeoff, moving the pipette away from the substrate often meant that the droplet looks smaller and it leads to greater doubt in water contact angle results. As a result, it was found that approximately 1.2 cm between the pipette and substrate can maximize droplet size thus preventing condensation as shown in Figure-2.

Image processing was done using ImageJ software to highlight the process involved by dragging a line between the edge of the water droplet for both right and left side. It allows the image to be processed into data. The picture is then cropped to eliminate any reflection from the substrate and tilted to the position where the substrate at the bottom of the screen. The effect of

roughness on wetting properties was analyzed by using contact angle measurement for different material and roughness. The image in Table-2 shows the contact angle value, two seconds after distilled water was dropped. The result shows that rough surface produced higher hydrophobicity than a smooth surface. The highest hydrophobic material was recorded for rough paraffin surface which is  $117.48^\circ$ . It was followed by the rough aluminium surface which produces  $110.42^\circ$  of water contact angle. Meanwhile, polystyrene and acrylic exhibits hydrophobicity presented the contact angle of less than  $90^\circ$ . Although all surfaces been rough by the same sandpaper, there is a material that produced a big gap between the rough and smooth surface. The aluminium surface produced a water contact angle of  $68.75^\circ$  and after the surface roughing process, the contact angle becomes  $110.42^\circ$ . This condition makes the aluminium surface has the biggest gap different which is  $41.67^\circ$ . Surface energy is the factor that affected the differences in contact angle between four types of specimens. Surface energy is the molecules on a solid substrate are affected by unbalanced molecular forces and therefore have additional energy in comparison to the molecules inside the solid. According to [22-24], surfaces with high surface energy will try to lower their energy by adsorbing low energy materials such as hydrocarbons. The surface energy showed in Table-2 are based on observation done by James [25]. From the finding, it shows in Table-2 that paraffin wax has low surface tension and high hydrophobicity among other specimens before roughness process occur. From the result, the hydrophobicity behaviours of paraffin surface can benefit used to repel water in certain applications. Surface energy for polystyrene and paraffin are less than  $40 \text{ mJ m}^{-2}$ , meanwhile, aluminium and acrylic recorded  $41 \text{ mJ m}^{-2}$  and  $169 \text{ mJ m}^{-2}$  for the surface energy. The lower surface energy of materials attributes to the higher contact angle.

**Table-2.** Water contact angle image and surface energy.


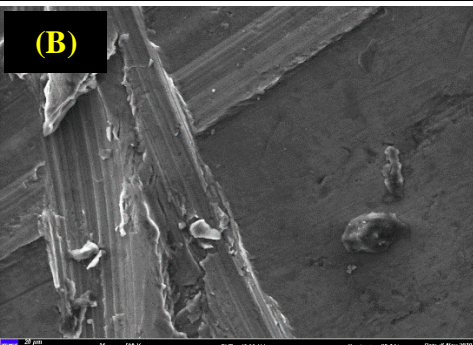
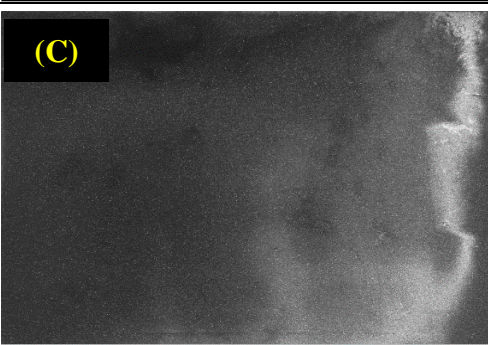
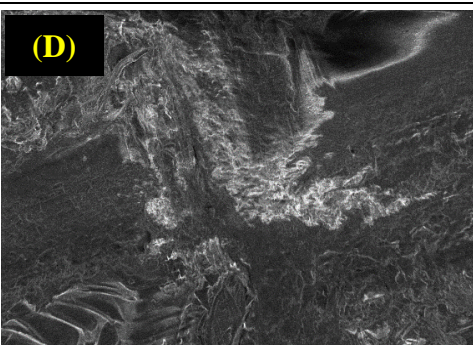
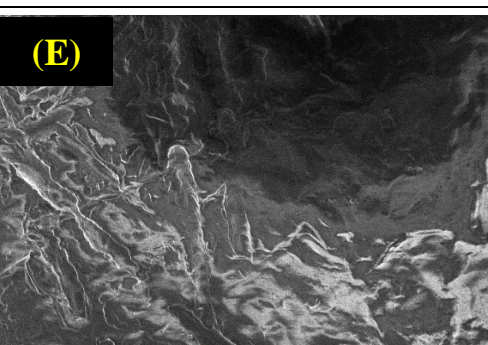
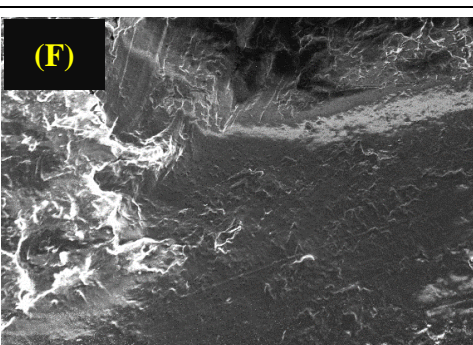
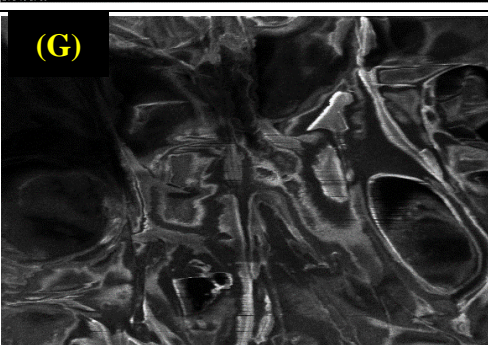
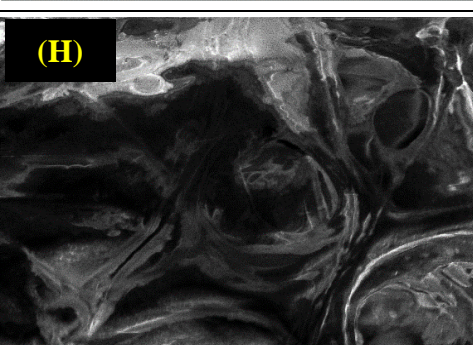
Specimens	Smooth Surface	Rough Surface	Surface Energy
Aluminium	(A)  68.75°	(B)  110.42°	169 mJ m <sup>-2</sup>
Paraffin	(C)  105.19°	(D)  117.48°	23 mJ m <sup>-2</sup>
Acrylic	(E)  63.25°	(F)  68.1°	41 mJ m <sup>-2</sup>
Polystyrene	(G)  71.9°	(H)  86.67°	33 mJ m <sup>-2</sup>

The scanning electron microscope (SEM) was used to characterize the morphology of the aluminium, paraffin, polystyrene and acrylic particles at 500X magnifications as shown in Table-3. After cutting and roughing of different material pieces, samples of the materials were taken individually for each block, and then the image was obtained separately for each sample. Table-3(A) shows that aluminium original smooth surface while it was cleaned, while Table-3(B) shows that rough surface of the aluminium. It can be seen that the smooth aluminium surface have less scratch when zooming at 500X magnifications. After the roughing process, the

aluminium surface has significant different roughness as the surface have larger cross-section scratch. By referring to the theory of Cassie-Baxter model, the peak and valley of the rough surface are more than the smooth surface, resulting in an increment of contact angle due to lack of air trap between the water and contact surfaces. This could be explained by Wenzel and Cassie-Baxter theory that elaborate the phenomena of a water droplet on a rough surface [26]. From SEM images of paraffin surface in Table-3(E) & (F), the smooth surface produces the highest water contact angle.



**Table-3.** Scanning electron microscope image before and after roughing process.

Specimens	Smooth Surface	Rough surface
Aluminium	 <p>(A)</p>	 <p>(B)</p>
Acrylic	 <p>(C)</p>	 <p>(D)</p>
Paraffin	 <p>(E)</p>	 <p>(F)</p>
Polystyrene	 <p>(G)</p>	 <p>(H)</p>

Based on Table-3(E) and 3(G), the smooth surface for paraffin and polystyrene have a tiny air pocket or air trap. This explained why both smooth material surface has the highest water contact angle than other materials. The smallest water contact angle came from a smooth acrylic surface. By referring to the SEM image of the smooth acrylic surface, the surface is flat with lesser

scratch compared to others. The surface roughness testing was carried out by using ISO 1997 standard. Based on the selected ISO 1997, the stylus probe was pulled for 5 mm in each sample. The results obtained in this study demonstrate the surface morphology of three materials against the arithmetical mean deviation (Ra) (Figure-3). Paraffin has the highest value for smooth and rough



surface compared to aluminium and acrylic. This result complies with the methodology used to obtain specimens roughness. Wetting is well proven to rely on surface morphology. The effect of roughness on the wetting properties was measured using water contact angle. Lowest contact angle but good wetting properties can be observed for the smooth acrylic surface with a contact angle of  $63.25^\circ$  as shown in table 2(E). It can be visualized that surface roughness was minimum when acrylic was used as the skimmer. Surface roughness was found minimum at the acrylic surface which has a value of 0.009 nm. The second smooth surface was shown by the aluminium surface which is 0.062. By referring to Figure-3, the smooth surface of paraffin there is only one obvious peak that produces 1.998 nm of Ra. The rough surface of paraffin showed the 3.49 nm of Ra which indicate the highest peak among other rough surfaces. The reason behind the paraffin behaviour was to a major extent. It is the product of the crystallizing forces proceeding to the plane layer, edges, and corners of crystals with a lot of holes and fissure due to the high degree of imperfection. Once a liquid droplet comes into contact with a smooth homogeneous solid surface, the droplet creates a uniquely defined equilibrium contact angle on top of a surface which is known as Young's relation. On the other example, 'if the same droplet is in interaction with a rough surface with a proper combination of surface texture and solid surface energy, the fluids may not completely penetrate the surface texture, but instead 'bead-up' to create a composite (solid-liquid-air) interface' [27]. The behaviours of the contact angle can be explained by using the Wenzel and Cassie-Baxter model. Cassie-Baxter model describes the relation of contact angle and surface roughness with air trap and the model can be expressed as Equation (1).

From the 2D profile of rough paraffin as shown in Figure-4, the increase of P-V causes the roughness of the surface to increase. But when the increase of D and W caused the contact angle to decrease due to less air trap between the surface thus allowing the liquid to penetrate easily between the P-V as depicted in Wenzel and Cassie-Baxter model. Compared to the smooth paraffin surface, the P-V less than the rough surface structure hence caused the contact angle to decrease due to lack of air trap between the water and contact surfaces. The experiment for retention time was conducted by preparing 3000 ml of water and 200 ml of oil. The mixture poured into the grease trap. There were 8 samples prepared that acts as oil skimmer. The sample divided into two groups that present a smooth and rough surface area of skimmers. The results have taken based on the volume mixture of oil and water after whole skimming process. The skimming process was set to 120 seconds as the skimmer start to collect oil from the container.

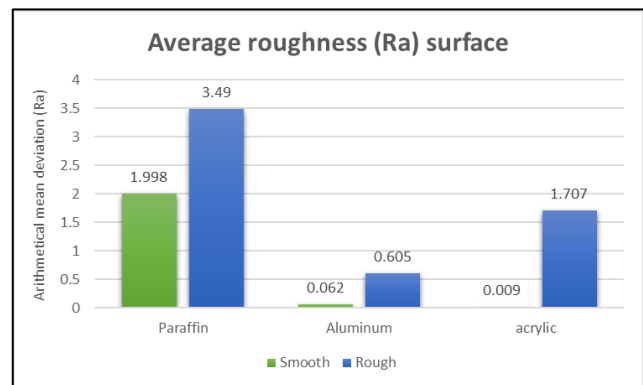


Figure-3. Average surface roughness.



Figure-4. Surface roughness of rough paraffin surface.

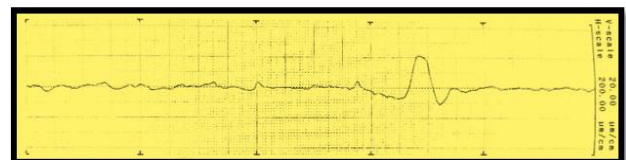


Figure-5. Surface roughness of smooth paraffin surface.

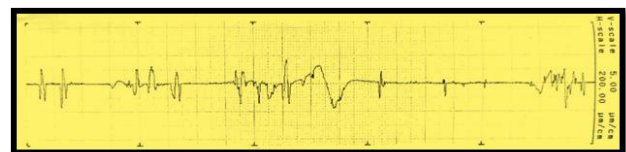


Figure-6. Surface roughness of rough aluminium surface.

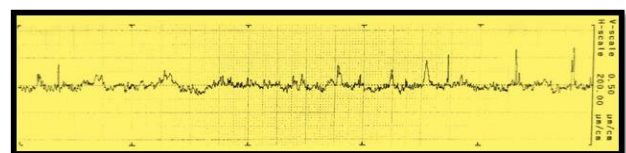


Figure-7. Surface roughness of smooth aluminium surface.

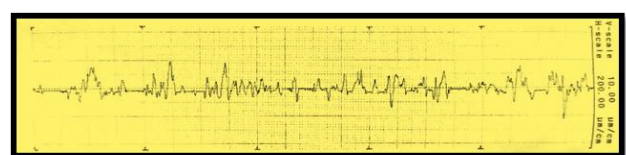
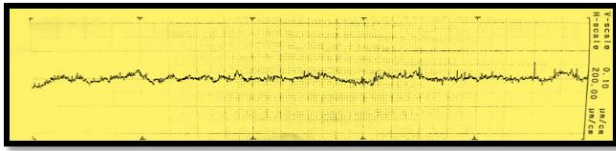


Figure-8. Surface roughness of rough acrylic surface.



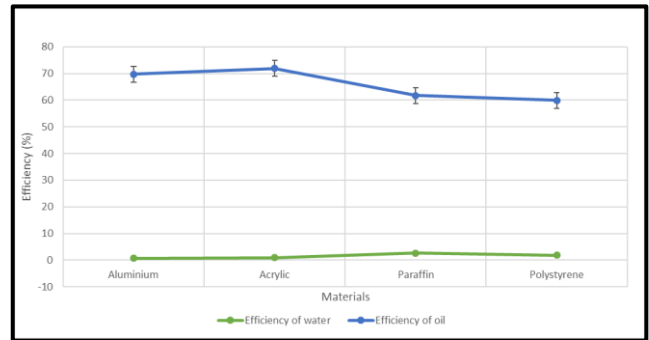
**Figure-9.** Surface roughness of smooth acrylic surface.  
 $\cos \theta_w = R_f \cos \theta_o - f_{LA}(R_f \cos \theta_o + 1)(1)$

**Table-4.** Oil-water skimming process (smooth surface).

Material	1 <sup>st</sup> test		2 <sup>nd</sup> test		3 <sup>rd</sup> test	
	Volume of Water (ml)	Volume of Oil (ml)	Volume of Water (ml)	Volume of Oil (ml)	Volume of Water (ml)	Volume of Oil (ml)
Aluminium	23.5	140	22.0	138	24.0	137
Acrylic	28.5	142	26.5	141	27.5	145
Paraffin	85.5	119	78.5	118	80.0	120
Polystyrene	58.3	116	54.0	117	56.5	115

**Table-5.** Oil-water skimming process in % (smooth surface).

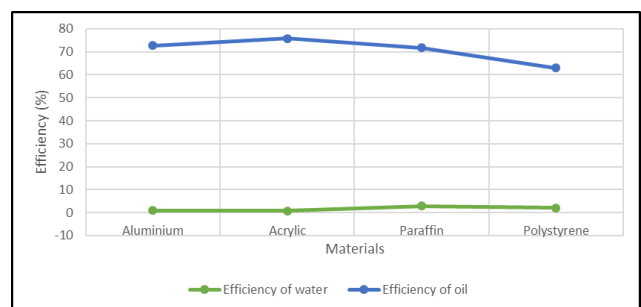
Material	1 <sup>st</sup> Test (%)		2 <sup>nd</sup> Test (%)		3 <sup>rd</sup> Test (%)		Average (%)	
	Water	Oil	Water	Oil	Water	Oil	Water	Oil
Aluminium	0.8	69.8	0.7	69.0	0.8	68.3	0.76	69.0
Acrylic	1.0	71.0	0.9	70.3	0.9	72.3	0.91	71.0
Paraffin	2.9	59.5	2.6	58.5	2.7	60.0	2.71	59.0
Polystyrene	1.9	57.8	1.8	58.0	1.9	57.3	1.87	58.0



**Figure-10.** Efficiency of skimmer for smooth material.

Based on Table-5, it can be seen that paraffin has the lowest efficiency as the skimmer collect the most water in the container. The number of collected water for paraffin skimmer is 2.71% or the 81.3-litre average of water. The lowest percentage of water that collected was collected from the aluminium material skimmer. This behaviour of this result is because aluminium has a higher surface roughness (Ra) than the acrylic. The most efficient skimmer for a smooth surface is made from acrylic. Results shown in Table-5, indicate that average of collected oil for an acrylic skimmer is the higher than other skimmers with aluminium is the second best. The different value between both materials are really small as the oil can be collected by using acrylic is 71% and 69% for the aluminium skimmer. Aluminium has minimum value compared to the acrylic. Acrylic is a better choice among other material because of the reliability and cheaper cost. From the observation for polystyrene material, it not suitable because polystyrene surface easily to scratch when contact with other abrasive materials.

Based on Table-6, the acrylic material produced a higher efficiency, with aluminium again drop to second place for a rough surface. For acrylic skimmer, the average oil percentage after skimming process can up to 75% and the oil that mix in the same beaker only 0.75% or 22.5 ml. The aluminium skimmer also has good efficiency as the result not far from the acrylic skimmer. The aluminium skimmer collected 72% of oil in the container. It was just 3% different from the acrylic skimmer. The water that mixes in the beaker shows that 0.78% meanwhile 0.75% for the acrylic.



**Figure-11.** Efficiency of skimmer for rough material.



**Table-6.** Oil-water skimming process in % (rough surface).

Material	1 <sup>st</sup> Test (%)		2 <sup>nd</sup> Test (%)		3 <sup>rd</sup> Test (%)		Average (%)	
	Water	Oil	Water	Oil	Water	Oil	Water	Oil
Aluminium	0.8	72	0.8	71	0.8	72	0.8	72
Acrylic	0.7	75	0.7	74	0.8	76	0.8	75
Paraffin	2.9	70	2.8	68	2.9	69	2.8	69
Polystyrene	2.0	60	2.1	63	2.1	61	2.1	61

## CONCLUSIONS

Material selection is the most important process as the skimmer materials must have the ability to repel as much water from the container and able to absorb more oil. The material that has been chosen and fabricated for the project are aluminium, acrylic, polystyrene and paraffin. They were characterized by using water contact angle, scanning electron microscopic (SEM), and profilometer. Surface roughness testing revealed that as the roughness (Ra) increases, it could lead to the increasing number of water contact angle. From the experiment, rough material surface produced a high-water contact angle compared to the smooth surface. Rough paraffin surface generated the highest water contact angle which is 117.48° and followed by rough aluminium surface. The water contact angle increases as the number of surface energy decrease. The rough surface of acrylic showed the most efficient skimming efficiency compared to aluminium, polystyrene and paraffin. It collected approximately 75% oil and 0.8% water in the container for 120 seconds. The second-best skimmer is using aluminium. From the observation, aluminium skimmer collected approximately 72% oil and 0.8% of water.

## ACKNOWLEDGEMENTS

Authors would like to express gratitude to Universiti Teknikal Malaysia Melaka (UTeM), Universiti

Tenaga Nasional (UNITEN), and Ministry of Higher Education for financial support on part of this research.

## REFERENCES

- [1] Dannefer R., Williams D. A., Baronberg S. and Silver, L. 2012. Healthy bodegas: increasing and promoting healthy foods at corner stores in New York City. *American Journal of Public Health*. 102, no. 10 27-31.
- [2] Klaucaus E. And Sams K. 2018. Problems with fat, oil, and grease (FOG) in food industry wastewaters and recovered FOG recycling methods using anaerobic Co-digestion: a short review. *Key Engineering Materials*. 762, 61-68.
- [3] Fauziah S. H., Simon C. and Periathamby A. 2004. Municipal solid waste management in Malaysia - Possibility of improvement?. *Malaysian Journal of Science* 23, no. 2, 61-70.
- [4] Keener K. M., Ducoste J. and Holt L. M. 2009. Properties influencing fat, oil, and grease deposit formation. *Water environment Research*. 80, no. 12, 1241-1246.
- [5] Otsuka T., Yamazaki H., Ankyu E., Ahamed T., Anda M. and Noguchi R. 2020. Elucidation of the mechanism of blockage in sewer pipes by fatty acid deposition and suspended solid. *Water*. 12, 2291.
- [6] Nieuwenhuis E., Post J., Duinmeijer A., Langeveld J., Clemens F. 2018. Statistical modelling of Fat, Oil and Grease (FOG) deposits in wastewater pump sumps. *Water Research*. 135, 155-167.
- [7] He X., Iasmin M., Dean L.O., Lappi S. E., Ducoste J. J. and Reyes F. L. 2011. Evidence for fat, oil, and grease (FOG) deposit formation mechanism in sewer lines. *Environmental Science & Technology*. 45, no. 10, 4385-4391.
- [8] Wallace T., Gibbons D., O'Dwyer M. and Curran T. P. 2017. International evolution of fat, oil, and grease (FOG) waste management - a review. *Journal of Environmental Management*. 187, 424-435.
- [9] Chinwetkitvanich S. and Ektaku P. 2020. Reality in package on-site grease trap performance: success and failure in fog removal. *International Journal of GEOMATE*. 18(67): 156-161.
- [10] He X., Reyes F. L. and Ducoste J. J. 2017. A critical review of fat, oil, and grease (FOG) in sewer





- collection systems: challenges and control. *Critical Reviews in Environmental Science and Technology*. 47(13): 1191-1217.
- [11] Nidzamuddin M. Y., Juffrizal K., Mustapha F., Zulfattah Z. M., Tan C. F., Taha M. M., Hidayah I. and Hilwa M. Z. 2015. Case study of the effectiveness of passive grease trap for management on domestic kitchen waste water. *AIP Conference Proceedings*. 1660, 070024.
- [12] Hussin M. S. F., Shamsudin M. A., Jumaidin R., Zakaria A. A., Jenal N. 2018. Portable grease trap for wastewater management system: a conceptual design approach. *Journal of Advanced Research in Fluid Mechanics and Thermal Sciences*. 49(1): 18-24.
- [13] Firdaus H. M. S., Halyani M. Y., Abdullah M. I. H. C., and Rafi O. M. 2017. Flexible shield for impact resistant purpose: a conceptual design. *Proceedings of Mechanical Engineering Research Day*. 134-135.
- [14] Baran Z. and Yildiz M. S. 2015. Quality function deployment and application on a fast food restaurant. *International Journal of Business and Social Science*. 6(9): 122-131.
- [15] Jaiswal E. S. 2012. A case study on quality function deployment (QFD). *IOSR Journal of Mechanical and Civil Engineering*. 3(6): 27-35.
- [16] Hussin M. S. F., Mukhtar M. F., Tumari M. Z. M., Ali N. M., Damanhuri A. A. M., Hamdan N. S., Azlan K. A., and Tofrowaih K. A. 2020. Conceptual design and structure analysis of giromill vertical axis wind turbine under low wind speed. *Journal of Advanced Research in Fluid Mechanics and Thermal Sciences*. 75(2): 11-19.
- [17] Smith G., Troy T. J. and Summers J. D. 2008. Concept exploration through morphological charts: an experimental study. *Proceedings of the ASME 2006 International Design Engineering Technical Conferences and Computers and Information in Engineering Conference*. 4a, 495-504.
- [18] Hussin M. S. F., Jumaidin R., Ali N. M., Fauzi M. A., Saat S., Sadun A. S., Yassim H. M. and Ahmad E. Z. 2020. Conceptual design and structure analysis of savonius vertical axis wind turbine under low wind speed. *Journal of Advanced Research in Fluid Mechanics and Thermal Sciences*. 71(2): 178-187.
- [19] Huang G. Q. and Mak K. L. 1999. Web-based morphological charts for concept design in collaborative product development. *Journal of Intelligent Manufacturing*. 10, 267-278.
- [20] Frey D. D., Herder P. M., Wijnia Y., Subrahmanian E., Katsikopoulos K. and Clausing D. P. 2009. The pugh controlled convergence method: model-based evaluation and implications for design theory. *Research in Engineering Design*. 20, 41-58.
- [21] Hussin M. S. F., Ahmad M. N., Maidin N. A., Rahman M. H. A., Ali N. M., Jumaidin R., Bakri J. and Rosli F. F. 2020. Risk factor analysis in fire fighter's posture with scutum-shaped shield including load and thermal exertion. *Journal of Physics: Conference Series*. 1529(4): 042037.
- [22] Mattox D. M. 2010. *Handbook of Physical Vapor Deposition (PVD) Processing*. Oxford, Elsevier.
- [23] Kozbial A., Li Z., Conaway C., Mcginley R., Dhingra S., Vahdat V., Zhou F., Urso B., Liu H. and Li L. 2014. Study on the Surface Energy of Graphene by Contact Angle Measurements. *Langmuir*. 30(28): 8598-8606.
- [24] Hefer A. W., Bhasin A. and Little D. N. 2006. Bitumen surface energy characterization using a contact angle approach. *Journal of Materials in Civil Engineering*. 18(6): 759.
- [25] Good R. J. and Girifalco L. A. 1960. A theory for estimation of surface and interfacial energies. III. Estimation of surface energies of solids from contact angle data. *The Journal of Physical Chemistry*. 64, no. 5. 561-565.
- [26] Simpson J. T., Hunter S. R. and Aytug T. 2015. Superhydrophobic materials and coatings: a review. *Rep Prog Phys*. 78(8), 086501.
- [27] Dettre R. H. and Johnson R. E. 1964. Contact angle hysteresis II. Contact angle measurements on rough surfaces. *Advances in Chemistry*. 43, 136-144.